Supporting information

A Biosensor Based on 3D-DNA Walking Machine Network and Distance-controlled Electrochemiluminescence Energy Transfer for Ultrasensitive Detection of Tenascin C and Lead Ion

Zi-Qi Xu, Pu Zhang, Ya-Qin Chai, Hai-Jun Wang*, Ruo Yuan*

Key Laboratory of Luminescent and Real-Time Analytical Cemistry, Ministry of Education, College of Chemistry and Chemical Engineering, Southwest University, Chongqing 400715, People's Republic of China.

* Corresponding author. Tel.: +86-23-68252277; Fax: +86-23-68253172.

E-mail address: hjwang@swu.edu.cn (HJ. Wang); yuanruo@swu.edu.cn (R. Yuan)

Reagents and materials

Human tenascin-c (TNC), biotin-antibody, avidin and the corresponding diluent were purchased from Elabscience Bio. Co. Ltd. (Wuhan, China). Cardiac troponin T antigen (cTnT) was made by Huayi Ltd., (Shanghai, China) and mucin 1 (MUC1) was provided by North Connaught Biotechnology Co. Ltd. (Shanghai, China). DNA in this work was obtained from Sangon Biotech Co., Ltd. (Shanghai, China) and listed as Table S1. Hexanethiol (HT), Tris-(2-carboxyethyl)-phosphine hydrochloride (TCEP) and gold chloride ($HAuCl_4 \cdot 4H_2O$) were provided by Sigma (St. Louis, MO, USA). Lead nitrate ($Pb(NO_3)_2$), $NaBH_4$, $(CH_3COO)_2Mn \cdot 4H_2O$ and Na_2S were purchased by Chemical Reagent Co. (Chongqing, China). Cadmium chloride hemipentahydrate ($CdCl_2 \cdot 2.5H_2O$) was obtained from Alfa Aesar Chemical Co., Ltd. (Tianjin, China). NH_2-Fe_3O_4 magnetic microspheres were purchased from Tianjin BaseLine ChromTech Research Centre (Tianjin, China). The phosphate-buffered solution of detection (0.1 M PBS, pH 7.0) and DNA hybridization buffer solution (10 mM Tris-HCl, 1.0 mM EDTA, and 1.0 M $MgCl_2$, pH 7.4) were prepared on the basis of the previous work.[1]

Table S1. The sequences of DNA used in our work

DNA	DNA sequence (5' to 3')
H1	NH_2-TCC TAC ACA TTC GTA CTT TGA CAG GAT CTA GTC TTG CCA TTA TGA CCA TCG ACA TCA TAG CTA ACT ATT GCA CAC ACT C
H2	NH_2-GAG TGT GTG CAA TAG TTA GCT ATG ATG TCG ATG GTC ATA ATG GCA AGA CTA GAT CCT GTC AAA GTA CGA ATG TGT AGC T
S1	NH_2-TTT GTA GAG AAG TTG AGT GAT AAA GCT GGC CGA GCC TCT TCT CTA CGC ACA CTA C-SH
S2	CGT AGA GAA GGA TAT CAC TCA A
W1	SH-TTT TTT TTT TTT TTT TTT TTT TTT TTT TTT TTT TTT TTT TTT TTT TTT TTT TTT TTT TTT TTT TTT GTA GTG TGC TTG GAG TGT TTT TTT TTT TTT TTT-Biotin
W2	Biotin- TTT TTT TTT TTT TTT TCA CTC CGT AGA GAA G

Apparatus

Electrochemical impedance spectroscopy (EIS) was carried out on a CHI 660A electrochemistry work station (Shanghai CH Instruments, China) and used the traditional three electrode electrochemical system with the working electrode of a modified glassy

carbon electrode (GCE, Φ = 4 mm), the auxiliary electrode of a platinum wire and the reference electrode of a saturated calomel electrode (SCE). ECL emission was monitored on a MPI-E ECL analyzer (Xi'an Remax Electronic Science & Technology Co. Ltd., Xi'an, China), with photomultiplier tube of 800V and potential scan from -1.5 V to 0 V. The surface appearances of nanocomposites were characterized by transmission electron microscope (TEM) and high resolution transmission electron microscopy (HRTEM, Tecnai G2 F20, FEI, USA).

Preparation of nanocomposites

Synthesis of AuNPs@Fe_3O_4

A typical method for synthesizing of AuNPs@Fe_3O_4 was showed as below. 500 μL magnetic microspheres (NH_2-Fe_3O_4) was washed with ultrapure water for three times and then added into 10 mL gold nanoparticles (AuNPs) which were prepared on the basis of previous work.[2,3] After stirring for 1 h at 4 °C and magnetic separation with ultrapure water, the AuNPs@Fe_3O_4 was obtained and dispersed in 1 mL Tris-HCl for later use.

Preparation of CdS:Mn-S1

As for synthesizing of CdS:Mn QDs, $Cd(NO_3)_2 \cdot 4\ H_2O$ (0.1683 g) and $Mn(CH_3COO)_2 \cdot 4\ H_2O$ (0.0134 g) were firstly dissolved in 30 mL ultrapure water under stirring and heated to 70 ºC. Later, 30 mL freshly prepared Na_2S (0.1 M) solution was added into the above mixture with refluxing for 3 h to obtain an orange precipitate. After centrifugation and abstersion, the CdS:Mn QDs were obtained. To prepare the CdS:Mn-S1, 100 μL S1 (10 μM) was incubated at 95 ºC for 5 min and then cooled down to 23 ºC slowly. After that, the prepared S1 was slowly added into a mixture of 500 μL CdS:Mn QDs and 10 μL TCEP (10 mM) at 4 ºC for 16 h. Finally, the CdS:Mn-S1 was obtained with the formation of Cd-S bond between thiol on S1 and CdS:Mn QDs.

Preparation of Ab1-W1 and Ab2-W2

Ab1-W1 was prepared as follows. Firstly, 50 μL of 3 μM W1 was initially incubated with equal volume of streptavidin at 37 °C for 30 min. And then, 100 μL Ab1 antibody was added into the above mixture for 30 min. Lastly, the mixture was ultra-filtrated with 20000 MW cutoff membrane to remove the unreacted reagents and the obtained Ab1-W1

was dissolved in 100 μL PBS buffer (pH 7.4) for later use. The Ab2 labeled W2 (Ab2-W2) was prepared as the same steps.

Preparation of two kinds of 3D-DNA walking machine

The 3D-DNA walking machine contained H1 was prepared by the following steps. As shown in Scheme 1 A, 1 mL CdS:Mn-S1, 50 μL Ab1-W1 and 50 μL of 1.5 μM H1 were added into 1 mL AuNPs@Fe_3O_4. Then, the mixture was continuously stirred for 16 h at 4 ^oC. Later, 10 μL HT (1%) was added to block the uncombined site. After magnetic-separating with ultrapure water for three times to remove the unreacted materials, the 3D-DNA walking machine contained H1 were prepared and dispersed into 1 mL PBS buffer (pH 7.4). The 3D-DNA walking machine contained H2 was prepared as the same steps.

Fabrication of the ECL biosensor

The cleaned glassy carbon electrode (GCE) was firstly electrodeposited in 1% $HAuCl_4$ solution for an Au nanoparticle layer (DpAu) at potential of -0.2 V for 30 s. Later, 20 μL of 1.5 μM S1 was incubated onto the sensing platform for 12 h and then 10 μL HT (1%) was added to block the uncombined site. Subsequently, 20 μL mixture containing two kinds of 3D-DNA walking machines were modified on the electrode surface for 6 h to assemble the network structure through base-pairing of H1 and H2. The AuNPs were now close to CdS:Mn QDs to quench the ECL signal ("off" state). Then, 20 μL of the target TNC and 20 μL of the prepared Ab2-W2 were incubated on the electrode for 30 min in turn. In this case, TNC combined Ab1-W1 and Ab2-W2 to generate walker for opening the CdS:Mn QDs labeled hairpin DNA S1 (the composite of walker-S1 dsDNA). Later, 20 μL S2 (1.5 μM) was added to fully hybridize with S1 labeled on the AuNPs@Fe_3O_4, obtaining the S1-S2 double-strands DNA (dsDNA) with a recognition site of Pb^{2+}. At the same time, the walker was released from walker-S1 dsDNA to hybridize with another S1, realizing the mechanical locomotion of walker. With the formation of S1-S2 double-stranded DNA, the distance between AuNPs and CdS:Mn QDs was increased, which lead to an enhanced ECL signal for TNC detection due to the excited surface plasma resonance ("on" state). Finally, 20 μL different concentrations of target Pb^{2+} solution was modified on the sensing surface at 37 ^oC for 1 h to cleave S2,

which restore the hairpin structure of S1 for closing AuNP and CdS:Mn QDs, decreasing the ECL signal for Pb^{2+}detection according to Förster energy transfer ("off" state).

Material characterization and ECL property of AuNPs/CdS:Mn QDs system

Firstly, transmission electron microscope (TEM) and high resolution transmission electron microscopy (HRTEM) were respectively utilized to characterize the prepared AuNPs and CdS:Mn QDs. As shown in TEM image of Figure S1 A, the dispersive AuNPs presented globular structures with average size about 4.2 ± 1.0 nm, and from HRTEM image of Figure S1 B, the CdS:Mn QDs exhibited the clearly lattice fringes with average size of 5.0 nm, which indicated the successful preparation of AuNPs and CdS:Mn QDs. Besides, in order to prove the energy transfer between AuNPs and CdS:Mn QDs, the ECL emission spectra of CdS:Mn QDs and UV-vis absorption spectra of AuNPs were also studied. As we can see from Figure S1 C, a maximum ECL emission spectra of CdS:Mn QDs appeared at 525 nm and a maximum UV-vis absorption spectra of AuNPs was observed at 520 nm. Apparently, the ECL emission spectra of CdS:Mn QDs were massively overlapped with the UV-vis absorption spectra of AuNPs, which indicated that the ECL energy transfer would occur between CdS:Mn QDs and AuNPs.

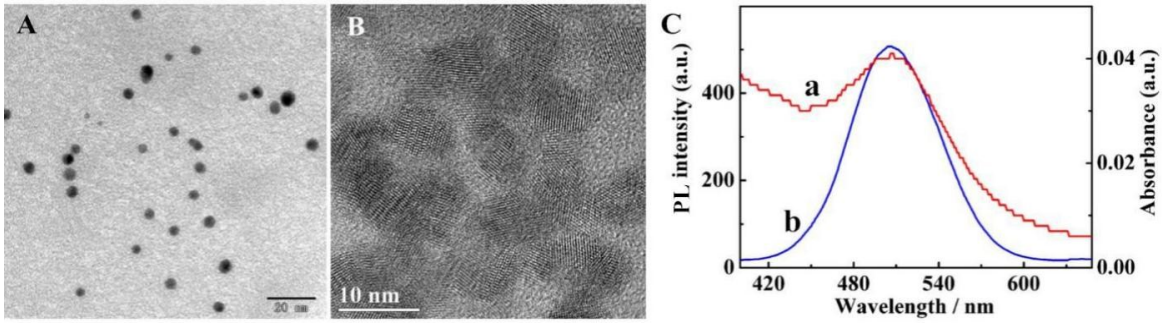

Figure S1 (A) TEM of AuNPs. (B) HRTEM of CdS:Mn QDs. (C) UV-vis absorption spectra of AuNPs (curve a) and ECL emission of CdS:Mn QDs (curve b).

Optimization of the experimental conditions on this ECL biosensor

The assembly efficiency of the 3D-DNA walking machine network was one of the important factors for the performance of ECL biosensor. Therefore, the assembly time of two kinds of DNA walking machines related to the assembly efficiency of the network was investigated. As seen in Figure S2 A, when the assembly time of the two kinds of DNA walking machines was increased from 2 to 7 h, the ECL signals accordingly

increased and attained a platform at 6 h. Therefore, 6 h was chosen as the appropriate assembly time of the two kinds of DNA walking machines in this system.

Moreover, the ratio of Ab1-W1 and S1 represents the ratio of walker and tracks assembled on Au@Fe_3O_4, which could considerably affect the walking efficiency of our walking machine. Therefore, the reaction ratio of Ab1-W1 and S1 was studied and the results were shown in Figure S2 B. When the ratio between Ab1-W1 and S1 shifted from 1:5 to 1:25, the increasing ECL signals could be observed and the maximum signal was reached at 1:20. Thus, the optimal ratio of Ab1-W1 and S1 was chosen as 1:20.

Besides, the reaction time of S2 caused great effect to the efficiency of distance-controlled energy transfer system, which further affected the sensitivity of the biosensor. Hence, the optimal reaction time of S2 was investigated under 100 fg mL^{-1} target TNC. As shown in Figure S2 C, the increasing ECL signals could be observed with the reaction time ranging from 40 to 140 min, and a maximum platform was reached at 120 min. Therefore, the appropriate reaction time of S2 was 120 min in this experiment.

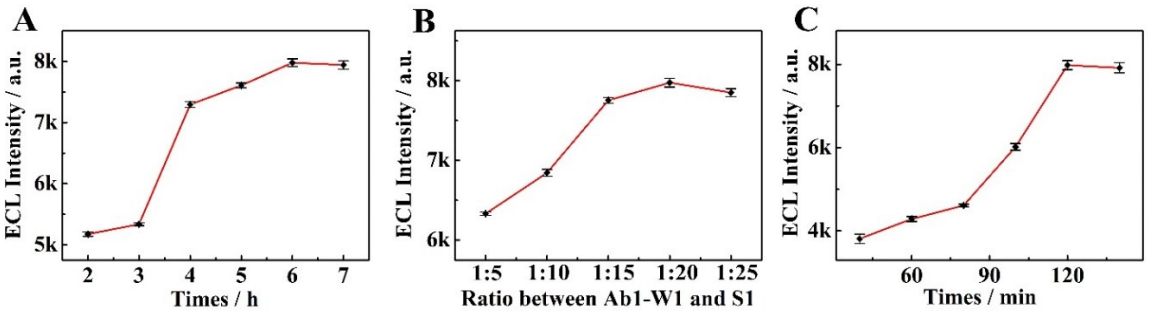

Figure S2. (A) The effect of the assembly time of the two kinds of DNA walking machines on the assembled efficiency of the 3D-DNA walking machine network. (B) The effect of reaction ratio of Ab1-W1 and S1 on the walking efficiency of the nanomachine. (C) The effect of the reaction time of S2 on the efficiency of distance-controlled energy transfer.

Table S2. Different methods for proteins and metal ions detection

analyte	methods	detection limit	dynamic range	references
cTnT	Nanofluidic Diode	10 fg mL^{-1}	1 fg mL^{-1} to 1 ng mL^{-1}	3
cTnI	ECL	0.016 pg mL^{-1}	0.05pgmL^{-1} to 0.10 ng mL^{-1}	4

TNC	Electrochemical	7 μg mL^{-1}	1 μg mL^{-1} to 100 μg mL^{-1}	5
	ECL	12.7 ng mL^{-1}	0.38 ng mL^{-1} to 24 ng mL^{-1}	6
	ECL	36.8 ag mL^{-1}	100 ag mL^{-1} to 1 ng mL^{-1}	This work
Pb^{2+}	Raman Scattering	1.8 ng mL^{-1}	20.7 ng mL^{-1} to 0.2 μg mL^{-1}	7
	Electrochemical	0.2 ng mL^{-1}	0.5 ng mL^{-1} to 100 ng mL^{-1}	8
	ECL	0.33 ng mL^{-1}	1 ng mL^{-1} to 1375 ng mL^{-1}	9
	ECL	0.8 fg mL^{-1}	2 fg mL^{-1} to 2 ng mL^{-1}	This work

For investigating the practical application of this system, the biosensor was employed in real samples for target TNC detection. Firstly, the real samples were prepared with diluted human serum which contained different concentrations of TNC (standard addition method). Then, the prepared samples were studied by the proposed biosensor. As we can see from Table S3, the recovery rates of these TNC samples were ranged from 97.07% to 101.70%, and the RSD was ranged from 1.480% to 3.591%, which indicated an excellent potentiality of the proposed biosensor in clinical detection of TNC.

Table S3. Recovery study of the biosensor with human serum

concentration of TNC/pg mL^{-1}	**concentration found/ pg mL^{-1}**	**recovery/%**	**RSD/%**
0.0001	0.00009707	97.07	1.480
0.01	0.009732	97.32	1.954
0.1	0.09782	97.82	2.441
10	10.17	101.7	3.591

References

1 Y. Zhou, H. J. Wang, H. Zhang, Y. Q. Chai, R. Yuan, *Anal. Chem*. 2018, **90**, 3543-3549.

2 M. X. Li, W. Zhao, G.S. Qian, Q. M. Feng, J. J. Xu, H. Y. Chen, *Chem. Commun.* 2016, **52**, 14230-14233.

3 Y. F. Liu, L. Yobas, *Nano Lett.* 2014, **14**, 6983-6990.

4 Z. Q. Xu, Y. W. Dong, J. Y. Li, R. Yuan, *Chem. Commun.* 2015, **51**, 14369-14372.

5 A. Steude, S. Schmidt, A. A. Robitzki, O. Panke, *Lab Chip*. 2011, **11**, 2884-2892.

6 S. Bhattacharyya, W. Wang, L. Morales-Nebreda, G. Feng, M. H. Wu, X. D. Zhou, R. Lafyatis, J. Lee, M. Hinchcliff, C. Feghali-Bostwick, K. Lakota, G. R. S. Budinger, K. Raparia, Z. Tamaki, J. Varga, *Nature Commun.* 2016, **7**, 11703-11714.

7 Y. Shi, H. Y. Wang, X. X. Jiang, B. Sun, B. Song, Y. Y. Su, Y. He, *Anal. Chem*. 2016, **88**, 3723-3729.

8 Q. W. Sun, J. K. Wang, M. H. Tang, L. M. Huang, Z. Y. Zhang, C. Liu, X. H. Lu, K. W. Hunter, G. S. Chen, *Anal. Chem*. 2017, **89**, 5024-5029.

9 C.Y. Xiong, W. B. Liang, H. J. Wang, Y. N. Zheng, Y. Zhuo, Y. Q. Chai, R. Yuan, *Chem. Commun.* 2016, **52**, 5589-5592.